



Increasing flooding hazard in coastal communities due to rising sea level: Case study of Miami Beach, Florida



Shimon Wdowinski ^{a, *}, Ronald Bray ^a, Ben P. Kirtman ^a, Zhaohua Wu ^b

^a Rosenstiel School of Marine and Atmospheric Sciences, University of Miami, USA

^b Department of Earth, Ocean, and Atmospheric Science, Center for Ocean-Atmospheric Prediction Studies, Florida State University, USA

ARTICLE INFO

Article history:

Received 11 December 2015

Received in revised form

8 March 2016

Accepted 11 March 2016

Keywords:

Sea level rise

Flooding hazard

Tide gauge record

EEMD

Southeast Florida

ABSTRACT

Sea level rise (SLR) imposes an increasing flooding hazard on low-lying coastal communities due to higher exposure to high-tide conditions and storm surge. Additional coastal flooding hazard arises due to reduced effectiveness of gravity-based drainage systems to drain rainwater during heavy rain events. Over the past decade, several coastal communities along the US Atlantic coast have experienced an increasing rate of flooding events. In this study, we focus on the increasing flooding hazard in Miami Beach, Florida, which has caused severe property damage and significant disruptions to daily life. We evaluate the flooding frequency and its causes by analyzing tide and rain gauge records, media reports, insurance claims, and photo records from Miami Beach acquired during 1998–2013. Our analysis indicates that significant changes in flooding frequency occurred after 2006, in which rain-induced events increased by 33% and tide-induced events increased by more than 400%. We also analyzed tide gauge records from Southeast Florida and detected a decadal-scale accelerating rates of SLR. The average pre-2006 rate is 3 ± 2 mm/yr, similar to the global long-term rate of SLR, whereas after 2006 the average rate of SLR in Southeast Florida rose to 9 ± 4 mm/yr. Our results suggest that engineering solutions to SLR should rely on regional SLR rate projections and not only on the commonly used global SLR projections.

© 2016 Elsevier Ltd. All rights reserved.

1. Introduction

Flooding hazard due to sea level rise (SLR) is a global problem. It affects about 10% of the Earth's population, roughly 700 million people, who live in low-lying coastal areas (McGranahan et al., 2007). In the US alone, 3.7 million people are living on land within 1 m of high tide and are in high risk of coastal flooding (Strauss et al., 2012). Despite the global SLR problem, coastal flooding hazard is a local problem, due to local elevation and elevation change (subsidence) of coastal communities, regional variations in the rate of SLR (Nicholls and Cazenave, 2010), as well as possible exposure to storm surge induced by extreme weather events (Aerts et al., 2014).

Most assessments of coastal flooding hazard rely on spatial information of coastal communities, including elevation, infrastructure, and population, as well as on expected value of SLR (e.g., Kleinosky et al., 2007; Kirshen et al., 2008, e.g., Strauss et al., 2012). Such assessments provide useful, long-term forecast of the

expected hazard due to a 'static' increase of sea level. Some studies also include tide gauge records for estimating flooding hazard due to storm surge (e.g., Nicholls, 2004; Tebaldi et al., 2012) and changes in flooding frequency (e.g., Cooper et al., 2008). However to our knowledge, none of the coastal hazard studies accounts for rain-induced flooding hazard, which arise from reduced effectiveness of gravity-based drainage systems as sea level rises.

The US Atlantic coast is one of the most vulnerable areas to SLR due to its low elevation, large population concentrations, and economic importance. Further vulnerability arises from accelerating rates of SLR, which began in the early 2000's possibly due to the slowing down of the Atlantic Meridional Overturning Circulation (AMOC) (Yin et al., 2009; Sallenger et al., 2012; Ezer et al., 2013). The increasing sea level also resulted in a significant increase of accumulated flooding time along the US Atlantic coast in the past twenty years (Ezer and Atkinson, 2014). Some coastal communities, as Norfolk, Virginia, have already experienced an increase in flooding frequency over the past decade (Kleinosky et al., 2007; Ezer et al., 2013).

The low elevation and highly populated area of southeast Florida is considered highly vulnerable to SLR. Recently, the city of

* Corresponding author.

E-mail address: shimonw@rsmas.miami.edu (S. Wdowinski).

Miami has been identified as the economically most vulnerable city to SLR in the world (US National climate assessment (Melillo et al., 2014)). Heretofore, the effect of SLR has felt mostly in low-lying coastal communities, such as the City of Miami Beach and some sections of Fort Lauderdale. In this study we assess flooding hazard in Miami Beach, based on documented flooding events that occurred during the time period 1998–2013. Our analysis accounts for three flooding types (rain, tide and storm surge) and reveals a significant increase in tidal flooding frequency since 2006, but also in rain-induced flooding events. Our study also includes a time series analysis of local tide gauge records and a correlation study with high-resolution global climate model. These additional analyses indicate that the post-2006 increased flooding frequency in Miami Beach correlates well with rapid acceleration of SLR in southeast Florida, which may have induced by weakening of the entire Gulf Stream system, as proposed previously (e.g., Ezer et al., 2013).

2. Study area

The city of Miami Beach is built on a barrier island off the coast of southeast Florida (Fig. 1). Throughout its century-long history, the city was subjected to flooding, mainly caused by heavy rain or storm surge. In recent years, rain-induced events have become more frequent and tide-induced ('sunny sky') flooding events have increased typically in September–October, around or after the fall equinox. The tide-induced floods have affected mostly low-lying neighborhoods in the western part of the city, which were built on reclaimed mangrove wetlands. Both the rain- and tide-induced events have caused severe property damage and significant disruptions to daily life.

3. Multi-disciplinary datasets

In order to characterize the recent flooding history of Miami Beach, we examine temporal information from five independent datasets: tide gauge, rain gauge, media reports, insurance claims, and photo documentation. The tide gauge record is of the National Oceanographic and Atmospheric Administration's (NOAA) operated Virginia Key station, which is located 5 km southwest of Miami Beach (Fig. 1). The rain record is of the NOAA's station USW00092811 located within Miami Beach. A two-year data gap (2001–2002) in the NOAA station record was filled by data from the nearby Miami-2 station, operated by the South Florida Water Management District. Media reports were collected using Google search and other search engines. The insurance claim record is the Miami Beach subset of flooding insurance claims, which are mandatorily reported to Federal Emergency Management Agency (FEMA) by insurance companies. The locations of the reported claims are shown in Fig. 1b. The last dataset, photo documentation of flooding events, was acquired by the city of Miami Beach since 2009.

The Virginia Key tide gauge station started operation in 1994 and has delivered sea level height record with a 6-min sampling rate, which provides a full and detailed description of the twice-daily tide cycle (green line in Fig. S1). However, some of the station's early data is available only as in monthly average format. In this study we analyze a time series consisting of the highest daily tide record, which is reported by NOAA as HH. The data are presented in the North America Vertical Datum 88 (NAVD) datum. More information on the tide record is provided in the Supporting Information (Section S1).

We present the HH tide gauge and rain data in yearly time series, which allows comparison of seasonal variations and flooding occurrences from one year to another (Fig. 2, Section S2). Flooding

events are tagged based on three record types: media reports, insurance claims and Miami Beach photo documentation. Each record is independent and spans over a different time period. Media reports were collected using Google search and other search engines for 'Miami Beach flooding'; their record covers the entire time span of our study 1998–2013. The insurance claim data are a subset of flood insurance claims that insurance companies are required to report the FEMA upon triggering of property (not cars) flood claims. FEMA shares this record with various agencies at county, state, and federal levels. We obtained our record for the years 1998–2012 from the Miami-Dade County's Public Works and Waste Management office, which provided a subset of the dataset containing locations and times of claims. Due to the Privacy Protection Act, other claim details were not provided to us. The third tagging record is photo archive collected by the city of Miami Beach. These three datasets allow us to tag flooding events and relate them to high tide and/or heavy rain conditions.

4. Cross-reference analysis

The annual time series presented in Fig. 2 show the cross-reference analyses of four representative years. In 2003 no flooding event was recorded. The HH tide record did not exceed 40 cm and no major rain event occurred. In 2005, four flooding events were tagged by insurance claims. The first two events (6/5 and 6/20) occurred during rain events. The other two events occurred during the passage of hurricane Katrina (8/25) and Wilma (10/24) and were caused by storm surge. In 2009 four flooding events were tagged by insurance claims (6/5), media reports (6/5 and 9/17), and Miami Beach documentation (6/24 and 11/18). The first event was caused by heavy rain (>200 mm) that resulted in massive flooding and a high number of insurance claims (53). The second flooding event (6/24) occurred during heavy rain and high tide conditions. The last two events (9/17 and 11/18) occurred during high tide conditions (>40 cm) with no rain ('sunny-sky flooding'). In 2013 we documented six flood events, two caused by heavy rain (4/14 and 7/17), and the other four by high tide conditions. Three of these events occurred in the fall–winter, around or after the fall equinox (9/17, 10/17, and 12/3), when sea level in the Miami area is highest. Interestingly, a fourth tide event was documented in the spring (3/13), just before the spring equinox, which is the second peak of sea level in the study area. The complete cross-reference analysis, including the dates and sources of the tagged flooding events, is presented in the Supporting Information (Section S4).

The cross-reference analysis allows us to evaluate the annual number and the causes of the Miami Beach flooding events (rain, tide, storm, and unexplained). A summary of all annual events according to types is presented in Table 1 and displayed visually in Fig. 3. We first summarized all available records, which show a significant increase in flooding occurrences since 2007 (Fig. 3a). By dividing the flooding record into two 8-year long periods (1998–2005 and 2006–2013), it is easy to notice a significant increase in both rain- and tide-induced events. During the first period, we counted 9 rain and 2 tide events, whereas in the second period we counted 15 rain and 15 tide events, an increase of 66% in the number of rain events and 750% of tide events. The record also shows a decrease in the number of storm events from three events in the first period (1998–2005) to zero in the later period. As storm events occur during anomalously high sea level conditions caused by storm surge, they are not indicative of regular sea level conditions and, hence, were omitted from our analysis.

Because the Miami Beach documentation record covers only the last five years of the study period, events documented by this record might bias the statistics. Thus, we repeated the same analysis using only the media and insurance records (Fig. 3b). When

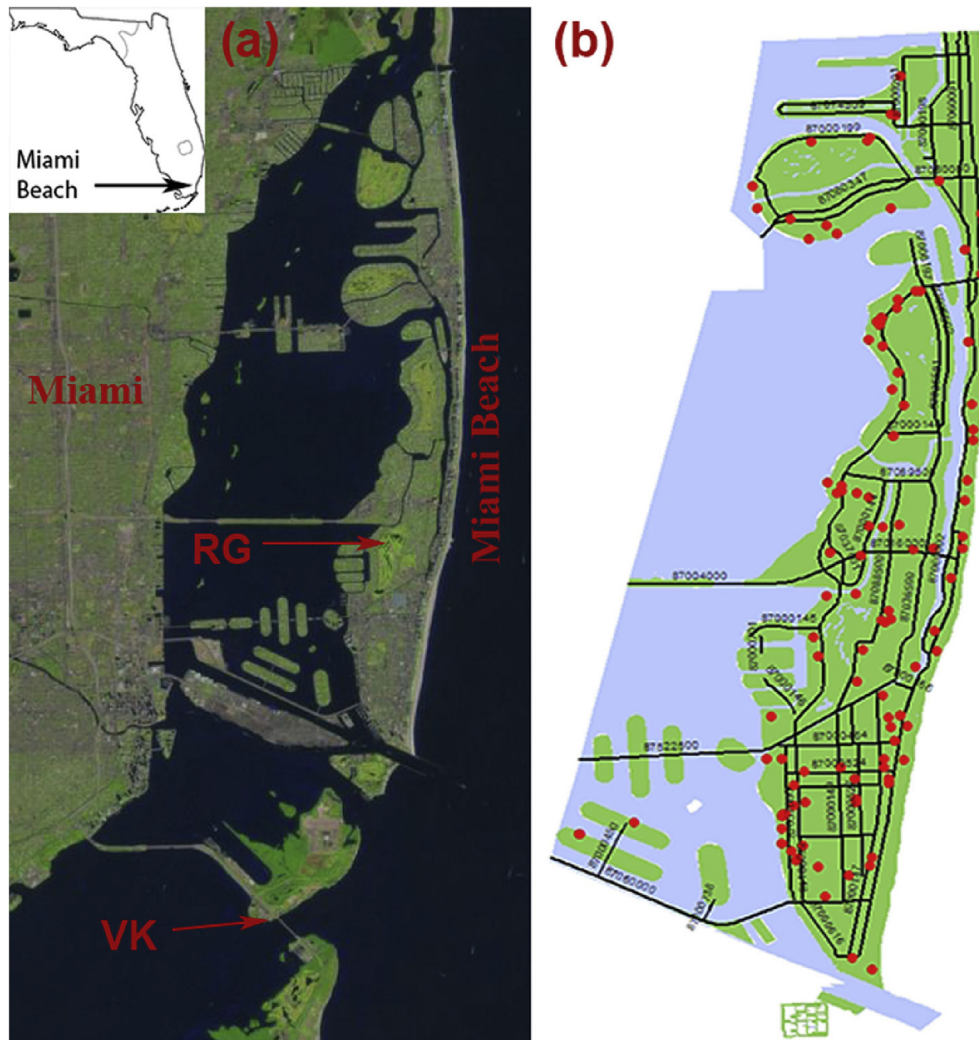


Fig. 1. (a) Landsat image showing the location of Miami Beach, the USW00092811 rain gauge (RG) and of the tide gauge station at Virginia Key (VK). Insert: Location map. (b) City map of Miami Beach showing the location of flood claims during the years 1998–2012.

omitting the Miami Beach documentation, the post-2006 increase of flooding events is not as high, but still apparent. The number of rain events increased from 9 events in the 1998–2005 time period to 12 events in the 2006–2013 period, an increase of 33%. A more significant increase appears in the number of tide events, from 2 to 8 events, an increase of 400%. Both analyses indicate a significant increase in tide-induced events after 2006.

A different approach for estimating the annual frequency of tidal flood events can be derived directly from the Virginia Key tide gauge record (Fig. 4a). We define that a tidal flooding event occurs when sea level reaches a certain threshold. In our cross-reference analysis, we found that tidal flooding threshold was in the range of 40–50 cm above the NADV datum. When using the 40 cm threshold, we detected a total of 119 events, in which 78 of them (65%) were in the period 2006–2013. When using 50 cm threshold, the number of detected events reduced significantly to 18, which is similar to the events detected by the cross-reference analysis (21 tide and storm events – Table 1). Again, most of the events using the 50 cm threshold (13 out of 18–72%) occurred after 2006. Three out of the pre-2006 events reflect storm surge events that occurred in 1999 and 2005. Over all, the tide gauge flooding analysis confirms the results of the cross-reference analysis in terms of distribution of events before and after 2006 and the four-fold

increase in number of flooding events during the 2006–2013 period compared to 1998–2005 (Fig. 4b).

5. Time series analysis of the Virginia Key tide gauge record

In order to evaluate the cause for the post-2006 increase of tide events, we analyze the 16-year long daily HH tide gauge record of the nearby Virginia Key station. Best-fit analyses of the tide gauge data reveal a high SLR rate, in the range of 4.1–4.9 mm/yr, depending on the assumed best-fit model (Fig. S2, Supporting Information, Section S2). Furthermore, when applying the best-fit model to subsections of the time series, the rate of SLR increases, which indicate an accelerating rate of SLR (Fig. S3).

An improved method for estimating the rate of SLR and its changes over time is the Ensemble of Empirical Mode Decomposition (EEMD) (Ji et al., 2014; Wu et al., 2009, 2011), which decomposes a time series naturally into amplitude-frequency modulated oscillatory components (often called modes). We applied the EEMD analysis to the Virginia Key daily HH time series and obtained twelve modes (Fig. S4). The high frequency modes correspond to sub-annual periodicities, whereas the low frequency modes correspond to the annual and multi-year periodicities. The last calculated mode is the trend, which represents the non-

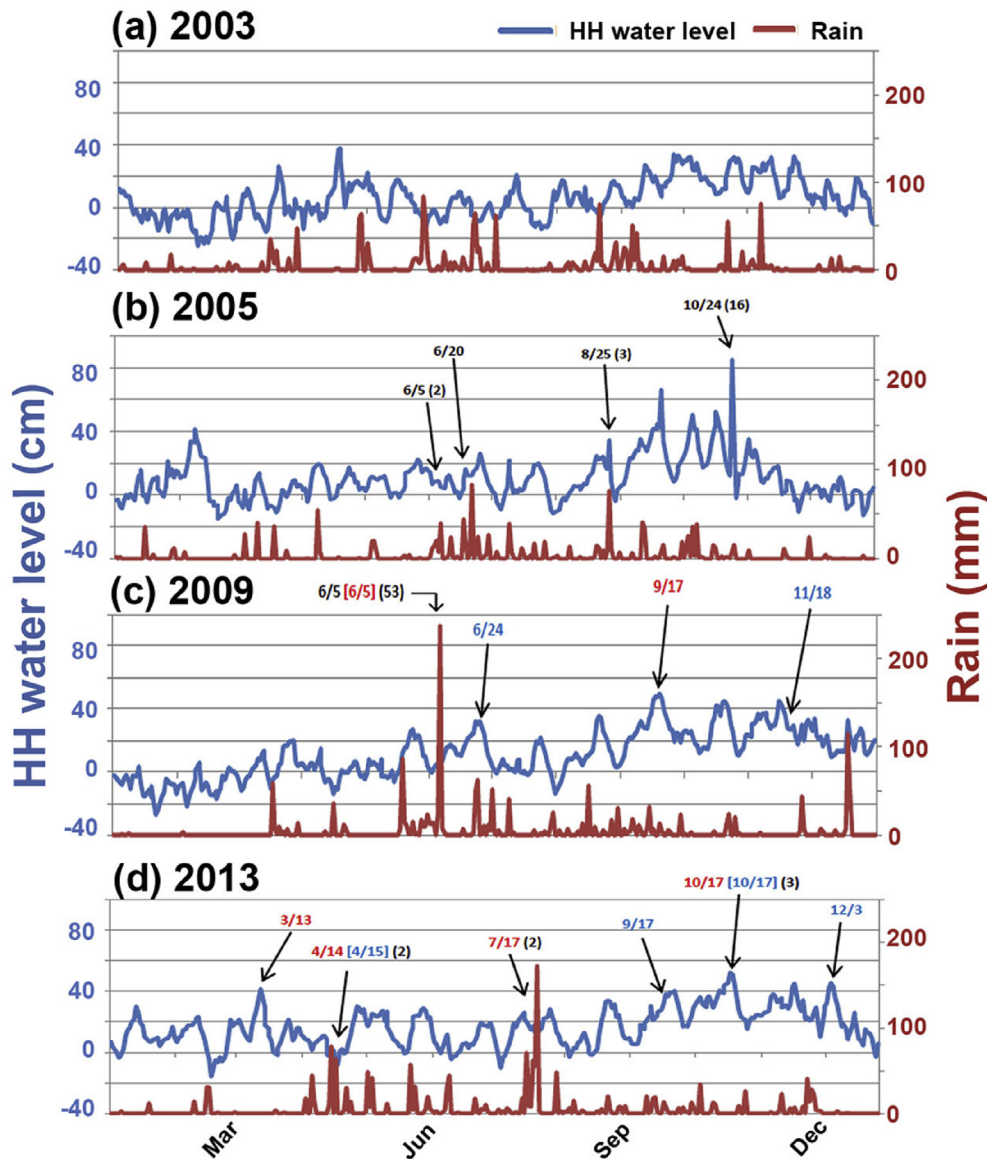


Fig. 2. Cross-reference analysis of Miami Beach flooding events using tide gauge (blue line), rain gauge (brown line), media reports (red text), insurance claims (black text), and Miami Beach documentation (blue text) records. The number in parentheses represents the number of reported claims. (a) Analysis of the 2003 data. No reported flooding. HH sea level never reached 40 cm (above NAVD). (b) Analysis of the 2005 data showing two rain events (6/5 and 6/20) and two storm events (8/25 – Katrina; 10/24 – Wilma). (c) Analysis of the 2009 data two rain events (6/5 and 6/25) and two tide events (9/17 and 11/18). (d) Analysis of the 2013 data showing two rain events (4/14 and 7/17) and four tide events (3/13, 9/17, 10/17, and 12/3). (For interpretation of the references to color in this figure legend, the reader is referred to the web version of this article.)

periodic change in the time series. The results of the EEMD analysis indicate an accelerating rate of SLR, which began around 2006 (Fig. 5). During this period of accelerated SLR, the HH level in Virginia Key rose by 8 ± 4 cm (Fig. S7), indicating an average rate of 9 ± 4 mm/yr since 2006. Our analysis also yielded the rate of SLR trend, indicating acceleration in the SLR rate from 3 ± 2 mm/yr in 2006 to 14 ± 5 mm/yr in 2013 (Fig. S7). However, these rates are instantaneous and do not reflect a long period of time. Thus, we prefer using the average of 9 ± 4 mm/yr for the period 2006–2013.

Park and Sweet (2015) analyzed monthly averaged tide gauge records of three southeast Florida sites (Virginia Key, Vaca key, and Florida Bay) using a similar Empirical Mode Decomposition (EMD) method. Their analysis revealed similar results indicating that the rate of SLR has accelerated from the long term 3.8–3.9 mm/yr to 5.9–7.4 mm/yr after 2003. They also analyzed the Florida Current transport record and found a 3 Sv decline in mean transport since

2006.

The results of our EEMD analysis, which indicates a significant acceleration in the rate of SLR since 2006, should be viewed cautiously because (1) the length of the time series, and (2) limitations of the EEMD method. Our time series analysis is based on a 16-year long Virginia Key tide gauge record. Such short tide gauge records are typically not used by long-term SLR studies, because they might be affected by nodal and other long-term cycles (18.61, 8.85, and 4.4 years) as well as by possible decadal-scale oceanic and atmospheric processes (e.g., Chambers et al., 2012). Despite the short length of the Virginia Key time series, the effect of nodal cycle on our estimate is minimal, because the dominant modulation along the US Atlantic coast is the 4.4-year quasi-lunar perigee cycle (Haigh et al., 2011), which has a limited bias on 16-year long time series. Unlike other studies concerning with the long-term SLR rate (e.g., Church and White, 2011), our study focuses on decadal scale

Table 1

Number of annual flooding events when using all data sources. The numbers in parentheses were calculated using only the Claim and Media records.

Year	Rain	Tide	Storm	Unexplained	Total	Summary
2013	2 (2)	4 (2)	0	0	6 (4)	2006–2013
2012	2 (1)	2 (2)	0	1	4 (3)	Rain: 15 (12)
2011	2 (1)	4 (0)	0	1 (1)	7 (2)	Tide: 16 (8)
2010	3 (3)	2 (1)	(0)	0	5 (4)	Storm: 0
2009	2 (1)	2 (1)	0	0	4 (2)	Unexp: 2 (2)
2008	1	1	0	0	2	Total: 33 (22)
2007	3	1	0	0	4	
2006	0	0	0	1	1	
2005	2	0	2	0	4	1998–2005
2004	1	1	0	0	2	Rain: 9
2003	0	0	0	0	0	Tide: 2
2002	2	0	0	0	2	Storm: 3
2001	0	0	0	0	0	Unexp: 2
2000	2	0	0	0	2	Total: 16
1999	1	1	1	2	5	
1998	1	0	0	0	1	

2004, which agree with EEMD results. Similar comparisons between EMD and other fitting methods for detecting SLR acceleration found good agreement between results obtained by the different methods (Ezer, 2013).

We have looked how SLR in the Miami area relates to the large-scale ocean circulation (Fig. 6) from available observational estimates of gridded surface currents in the Atlantic Oceans (Ocean Surface Current Analyses – Real time; OSCAR; www.oscar.noaa.gov) (Johnson et al., 2007) and from a very high resolution global climate model simulation (Kirtman et al., 2012). The model results (shading in Fig. 6) indicate that a weakening of the entire Gulf Stream system (decrease in kinetic energy) is correlated with increasing sea level in the Miami area. However, available gridded observational estimates of the surface currents (contours) do not appear to be consistent with a weakening with the entire Gulf Stream system.

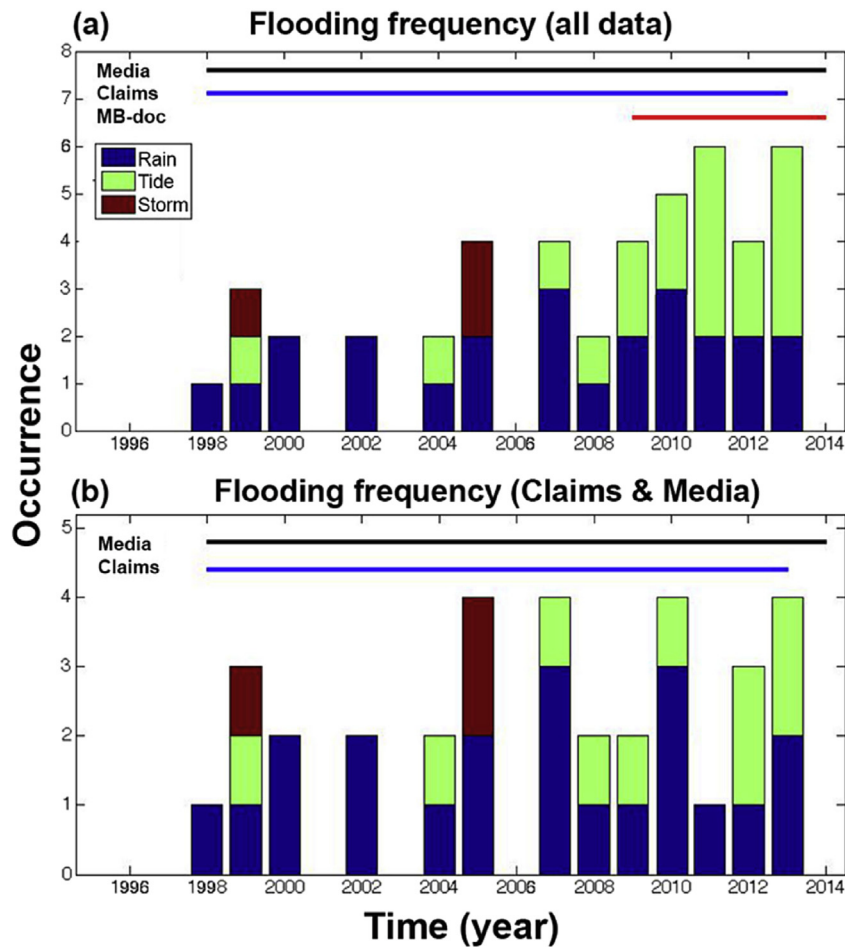


Fig. 3. Flooding frequency in Miami Beach when all data sources are used (a) and with partial data that cover most of the time span (b).

variations in the rate of SLR. Thus, the 16-year length of the Virginia Key time series is suitable for such analysis.

The limitation of the EMD and EEMD methods was pointed out by Chambers (2015), who found that such methods could perform poorly when detecting climate modes or accelerations. In order to evaluate the performance of the EEMD results, we estimated the acceleration using a second-order polynomial least-square fit and obtained acceleration rate of 0.076 mm/yr² and a minima around

6. Discussion

Our multi-disciplinary coastal flooding hazard analysis differs from most other coastal flooding hazard studies in terms (1) time period, (2) consideration of rain-induced flooding events, and (3) reported results. Most assessments of coastal flooding hazard evaluate future exposure of coastal communities to a 'static' increase of sea level and report their results according to inundated

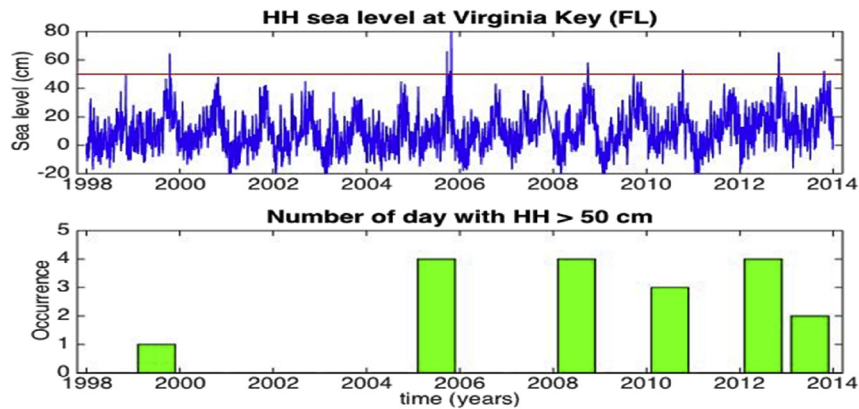


Fig. 4. Tidal and storm flooding events based the Virginia Key (VK) tide gauge record with threshold of 50 cm above the NAVD datum (horizontal red line) (a). A histogram of flooding occurrence showing a significant increase in annual occurrence after 2006 (b). (For interpretation of the references to color in this figure legend, the reader is referred to the web version of this article.)

area or affected population size (e.g., Kleinosky et al., 2007; Kirshen et al., 2008, e.g., Strauss et al., 2012). These studies calculate

increasing sea level in south Florida correlates with weakening of a long section of the Gulf Stream system (decrease in kinetic energy

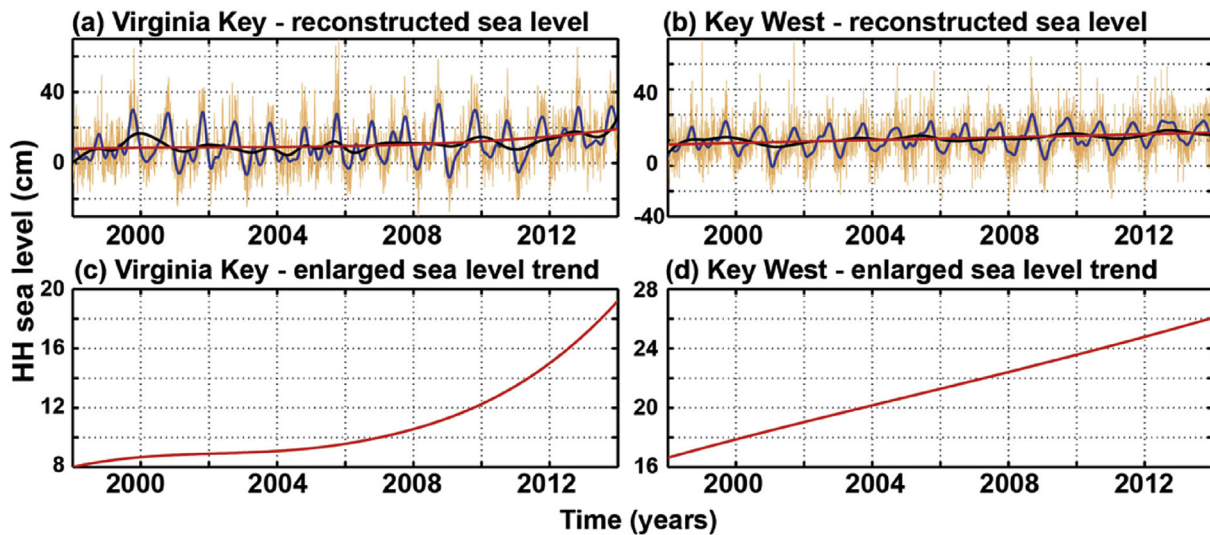


Fig. 5. EEMD analysis of the Virginia Key and Key West HH sea level records for the period 1998–2013. Lines: brown - original series; blue – annual component; black – multi-year component; red – trend. (For interpretation of the references to color in this figure legend, the reader is referred to the web version of this article.)

flooding hazard induced by high tide and/or storm surge, but not due to rain events. Our study is based on documented past flooding events, which occurred during a 16-year period and were induced by all three sources: high tide, storm surge and rain. Furthermore, we report our hazard results in terms of annual flooding frequency, which reflects the gradual transition of a dynamic sea level surface from 'dry' to 'completely inundated' land.

Including rain-induced events in our analysis revealed that such events impose a significant hazard, as they occur in the sub-tropical climate of Miami Beach 2–3 times per year (Fig. 3 and Table 1). We also found that increasing sea level also increased the frequency of rain-induced flooding events by 33%, because of higher sea level reduces the effectiveness of gravity-based drainage systems. In 2014, the city of Miami Beach invested millions of dollars replacing some of the ineffective gravity-based drainage system by a pumped-based system. Indeed, the change to pump-based drainage system resulted in reduced flooding events in the city.

Our high-resolution climate modeling results indicate that

– Fig. 6). These findings support the results of recent studies suggesting that decadal-scale accelerating rates of SLR along most of the US Atlantic coast have occurred due to the weakening of AMOC (Ezer, 2013; Ezer et al., 2013; Ezer and Corlett, 2012; Sallenger et al., 2012; Yin et al., 2009; Park and Sweet, 2015). However, the acceleration along most of the US Atlantic coast began around 2000 (Ezer, 2013), whereas the acceleration in the Miami area was delayed and began after 2006. In order to verify that the acceleration starting point in the Virginia Key record is different than other locations, we conducted EEMD analysis of the following four South and Central Florida tide records: Virginia Key, Key West, Trident Pier (Cape Canaveral), and Naples (Fig. S7). Our analysis indicates that the rate of SLR in the two Gulf of Mexico stations (Key West and Naples) is moderate (5–6 mm/yr) and rate of change is almost linear, suggesting that the acceleration began before 2000 (Fig. 4 and Fig. S7). The analysis of the two Atlantic stations (Virginia Key and Trident Pier) indicates delayed accelerations in which the acceleration began after 2006. The delayed SLR acceleration in the

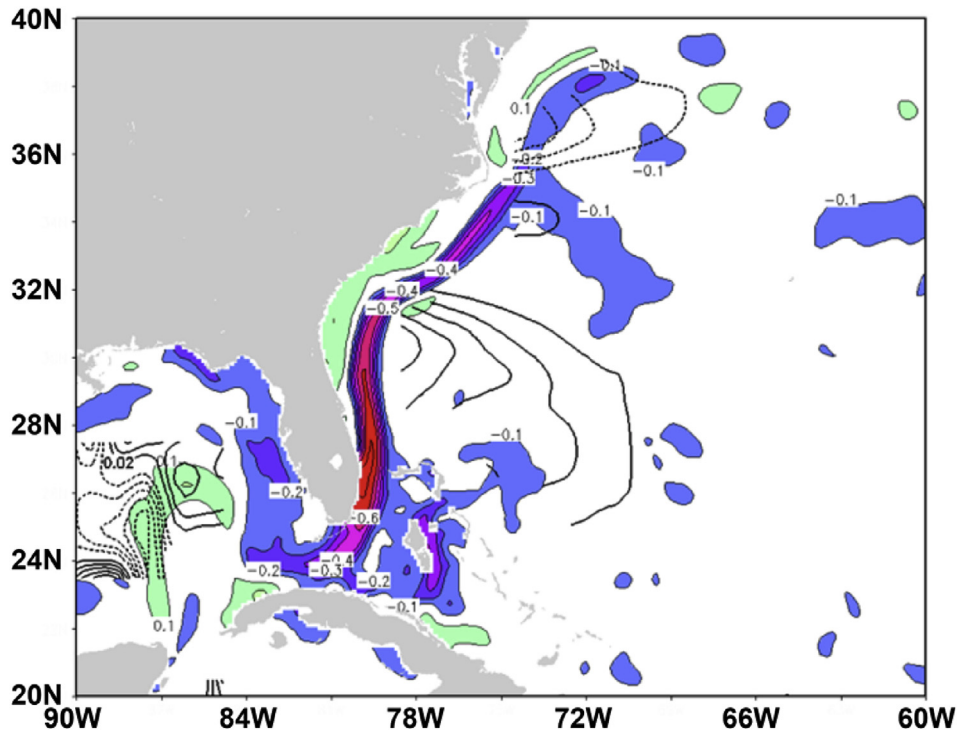


Fig. 6. Shading shows the correlation between sea level variation at the grid point nearest to Miami Beach and the ocean surface kinetic energy. The correlation is calculated from a last 50-years of 150-year very high resolution (~10 km) global coupled climate model simulation with greenhouse gas concentrations fixed at 1990 levels (Kirtman et al., 2012). The thick dashed and solid contours indicate the epochal meridional surface current difference (2004–present average minus 1993–2003 average). The thick contours are in m s^{-1} and dashed contours corresponds to negative values.

Miami area with respect to other sections of the US Atlantic coast may reflect a different dynamic response of the Florida Current than that of the Gulf Stream to climatic-induced changes to the AMOC and an associated weakening of the Gulf Stream.

7. Conclusions

The accelerated rate of SLR in Southeast Florida (9 ± 4 mm/yr since 2006) and other locations along the US Atlantic coast are significantly higher than the global average rate of SLR, which is estimated for the period of 1993–2012 from satellite data as 3.2 ± 0.4 and from in situ data as 2.8 ± 0.4 (Church et al., 2013). Many areas worldwide have experienced higher than the global average rates of SLR, sometimes as high as 20 mm/yr, as in the western Pacific Ocean (e.g., Nicholls and Cazenave, 2010). Spatial variability in the rate of SLR results from salinity variations, non-uniform ocean warming, changes in ocean circulation, and solid Earth's response to the last deglaciation, and changes in gravitational attraction due to ice melt (Stammer, 2008; Wunsch et al., 2007; Milne et al., 2009; Hay et al., 2015). Moreover, since a coherent decrease in the Gulf Stream has not been detected to date and since current climate change projects do predict a coherent decrease, our model results suggest that additional acceleration is possible. Therefore, it is extremely important to take into account the spatial variability in SLR when preparing a city, as Miami Beach, to adapt to increasing sea levels. Engineering projects, such as increasing efficiency of drainage systems or erection of seawalls, are typically based on globally average forecasts of SLR. Thus, if local rates of SLR are significantly higher than those of the globally average ones, as observed in Miami Beach, planned engineering solutions will provide protection for a shorter time period than planned.

Acknowledgments

We thank NOAA for providing the tide and rain gauge records. We are also thankful to Marcia Steelman (Miami-Dade County) for sharing with us the flood claim record, and to Elizabeth Wheaton, Margarita Wells, and Christine Borski (City of Miami Beach) for the Miami Beach flooding photo documentation. The research was supported by NASA's award number NNX13AP95G.

The tide and rain gauge data for this paper are available at NOAA's Center for Operational Oceanographic Products and Services (CO-OPS), under products/Water Levels and NOAA's National Climate Data Center under precipitations, respectively. Additional data for the cross-reference analysis are available at [Supporting Information Section S4](#).

Appendix A. Supplementary data

Supplementary data related to this article can be found at <http://dx.doi.org/10.1016/j.ocecoaman.2016.03.002>.

References

- Aerts, J.C.J.H., Botzen, W.J.W., Emanuel, K., Lin, N., de Moel, H., Michel-Kerjan, E.O., 2014. Evaluating flood resilience strategies for coastal megacities. *Science* 344.
- Chambers, D.P., 2015. Evaluation of empirical mode decomposition for quantifying multi-decadal variations and acceleration in sea level records. *Nonlinear Process. Geophys.* 22, 157–166.
- Chambers, D.P., Merrifield, M.A., Nerem, R.S., 2012. Is there a 60-year oscillation in global mean sea level? *Geophys. Res. Lett.* 39.
- Church, J.A., Clark, P.U., Cazenave, A., Gregory, J.M., Jevrejeva, S., Levermann, A., Merrifield, M., Milne, G., Nerem, R., Nunn, P., 2013. *Sea Level Change*. PM Cambridge University Press.
- Church, J.A., White, N.J., 2011. Sea-level rise from the late 19th to the early 21st century. *Surv. Geophys.* 32, 585–602.
- Cooper, M.J.P., Beevers, M.D., Oppenheimer, M., 2008. The potential impacts of sea level rise on the coastal region of New Jersey, USA. *Clim. Change* 90, 475–492.

- Ezer, T., 2013. Sea level rise, spatially uneven and temporally unsteady: why the US East Coast, the global tide gauge record, and the global altimeter data show different trends. *Geophys. Res. Lett.* 40, 5439–5444.
- Ezer, T., Atkinson, L.P., 2014. Accelerated flooding along the U.S. East Coast: on the impact of sea-level rise, tides, storms, the Gulf Stream, and the North Atlantic Oscillations. *Earth's Future* 2.
- Ezer, T., Atkinson, L.P., Corlett, W.B., Blanco, J.L., 2013. Gulf Stream's induced sea level rise and variability along the U.S. mid-Atlantic coast. *J. Geophys. Res. Oceans* 118, 685–697.
- Ezer, T., Corlett, W.B., 2012. Is sea level rise accelerating in the Chesapeake Bay? A demonstration of a novel new approach for analyzing sea level data. *Geophys. Res. Lett.* 39.
- Haigh, I.D., Eliot, M., Pattiaratchi, C., 2011. Global influences of the 18.61 year nodal cycle and 8.85 year cycle of lunar perigee on high tidal levels. *J. Geophys. Res. Oceans* 116.
- Hay, C.C., Morrow, E., Kopp, R.E., Mitrovica, J.X., 2015. Probabilistic reanalysis of twentieth-century sea-level rise. *Nat. Clim. Change* 5, 481–484.
- Ji, F., Wu, Z., Huang, J., Chassignet, E.P., 2014. Evolution of land surface air temperature trend. *Nat. Clim. Change* 4, 462–466.
- Johnson, E.S., Bonjean, F., Lagerloef, G.S.E., Gunn, J.T., Mitchum, G.T., 2007. Validation and error analysis of OSCAR sea surface currents. *J. Atmos. Ocean. Technol.* 24, 688–701.
- Kirshen, P., Knee, K., Ruth, M., 2008. Climate change and coastal flooding in Metro Boston: impacts and adaptation strategies. *Clim. Change* 90, 453–473.
- Kirtman, B.P., Bitz, C., Bryan, F., Collins, W., Dennis, J., Hearn, N., Kinter III, J.L., Loft, R., Rousset, C., Siqueira, L., Stan, C., Tomas, R., Vertenstein, M., 2012. Impact of ocean model resolution on CCSM climate simulations. *Clim. Dyn.* 39, 1303–1328.
- Kleinosky, L.R., Yarnal, B., Fisher, A., 2007. Vulnerability of Hampton Roads, Virginia to storm-surge flooding and sea-level rise. *Nat. Hazards* 40, 43–70.
- McGranahan, G., Balk, D., Anderson, B., 2007. The rising tide: assessing the risks of climate change and human settlements in low elevation coastal zones. *Environ. Urban.* 19, 17–37.
- Melillo, J.M., Richmond, T.T.C., Yohe, G.W., EDS, 2014. *Climate Change Impacts in the United States: the Third National Climate Assessment*. U.S. Global Change Research Program.
- Milne, G.A., Gehrels, W.R., Hughes, C.W., Tamisiea, M.E., 2009. Identifying the causes of sea-level change. *Nat. Geosci.* 2, 471–478.
- Nicholls, R.J., 2004. Coastal flooding and wetland loss in the 21st century: changes under the SRES climate and socio-economic scenarios. *Glob. Environ. Change Human Policy Dimens.* 14, 69–86.
- Nicholls, R.J., Cazenave, A., 2010. Sea-level rise and its impact on coastal zones. *Science* 328, 1517–1520.
- Park, J., Sweet, W., 2015. Accelerated sea level rise and Florida current transport. *Ocean Sci.* 11, 607–615.
- Sallenger, A.H., Doran, K.S., Howd, P.A., 2012. Hotspot of accelerated sea-level rise on the Atlantic coast of North America. *Nat. Clim. Change* 2, 884–888.
- Stammer, D., 2008. Response of the global ocean to Greenland and Antarctic ice melting. *J. Geophys. Res. Oceans* 113.
- Strauss, B.H., Ziemiński, R., Weiss, J.L., Overpeck, J.T., 2012. Tidally adjusted estimates of topographic vulnerability to sea level rise and flooding for the contiguous United States. *Environ. Res. Lett.* 7.
- Tebaldi, C., Strauss, B.H., Zervas, C.E., 2012. Modelling sea level rise impacts on storm surges along US coasts. *Environ. Res. Lett.* 7.
- Wu, Z., Huang, N.E., Chen, X., 2009. The multi-dimensional ensemble empirical mode decomposition method. *Adv. Adapt. Data Anal.* 1, 339–372.
- Wu, Z., Huang, N.E., Wallace, J.M., Smoliak, B.V., Chen, X., 2011. On the time-varying trend in global-mean surface temperature. *Clim. Dyn.* 37, 759–773.
- Wunsch, C., Ponte, R.M., Heimbach, P., 2007. Decadal trends in sea level patterns: 1993–2004. *J. Clim.* 20, 5889–5911.
- Yin, J., Schlesinger, M.E., Stouffer, R.J., 2009. Model projections of rapid sea-level rise on the northeast coast of the United States. *Nat. Geosci.* 2, 262–266.